Hyperfine Interact (2017) 238:103
https://doi.org/10.1007/s10751-017-1459-x

Effects of mechanical loading on the magnetic and dynamic properties of engineering materials

L. Scherthan[1] · H. Auerbach[1] · S. Deldar[2] · K. Jenni[1] · J. A. Wolny[1] · M. Herlitschke[3] · H.-C. Wille[3] · A. Mutter[4] · J. Meiser[4] · P. Umstätter[4] · H. M. Urbassek[4] · T. Beck[2] · M. Smaga[2] · V. Schünemann[1]

Abstract The influence of strain on the magnetic and dynamic properties of ARMCO iron has been characterized by Mössbauer spectroscopy and by Nuclear Inelastic Scattering of synchrotron radiation. The Mössbauer spectra, taken in backscattering geometry, reveal that the magnetic texture in these materials is depending on the type of mechanical loading, monotonic or cyclic, respectively. The applicability of Nuclear Inelastic Scattering for the investigation of the dynamic properties of these macroscopic bulk-engineering materials is shown. The so obtained phonon density of states of a monotonically loaded specimen shows slight differences in its shape and spectral features in comparison to the initial state. An influence of dislocations is also reflected in theoretically calculated phonon density of states based on classical molecular dynamics simulations.

Keywords Tensile test · Fatigue · ARMCO iron · Mössbauer spectroscopy · Nuclear inelastic scattering

This article is part of the Topical Collection on *Proceedings of the International Conference on the Applications of the Mössbauer Effect (ICAME 2017), Saint-Petersburg, Russia, 3–8 September 2017* Edited by Valentin Semenov

Electronic supplementary material The online version of this article (https://doi.org/10.1007/s10751-017-1459-x) contains supplementary material, which is available to authorized users.

✉ L. Scherthan
schertha@rhrk.uni-kl.de

[1] Department of Physics, University of Kaiserslautern, 67663 Kaiserslautern, Germany

[2] Institute of Materials Science and Engineering (WKK), University of Kaiserslautern, 67663 Kaiserslautern, Germany

[3] Deutsches Elektronen Synchrotron DESY, 22607 Hamburg, Germany

[4] Physics Department and Research Center OPTIMAS, University of Kaiserslautern, 67663 Kaiserslautern, Germany

Published online: 27 November 2017

1 Introduction

As fatigue is one of the most common reasons for failure of mechanical components of daily use, the detailed investigation of this phenomenon can lead to an optimization of the construction of more sustainable components [1, 2]. Consequently, an investigation of the magnetic and dynamic properties induced by mechanical monotonic and/or cyclic loading is of particular interest [3]. As a representative for ferromagnetic metallic materials, we examine ARMCO iron by Mössbauer spectroscopy to get insight in the static magnetic properties. Furthermore, as changes in dislocation density and arrangement play a crucial role for failure, we explore if such microstructural changes due to mechanical loading are reflected in the partial density of phonon states (pDOS) that can be determined via synchrotron based Nuclear Inelastic Scattering (NIS) [4, 5].

2 Materials and methods

In the current study, we have investigated polycrystalline ARMCO iron with body-centered cubic (bcc) structure, not enriched with ^{57}Fe, delivered by Allied Materials. ARMCO iron is the trade name of technically pure iron with a purity of 99.8 to 99.9%. The material was prepared as flat specimens with a gauge length of 6 mm and a cross section area of 6 mm $\times$ 6 mm (see Fig. 1). Monotonic and cyclic material tests were performed at ambient temperature. In-situ (during mechanical loading) and ex-situ (at definite deformation state) measurements with a Hall-sensor showed a thereby induced change in magnetic flux density [6]. In this way, five samples were delivered in order to explore the state just before and after failure due to monotonic and cyclic loading (see Table 1).

Regarding the monotonic loading, we previously reported about an observable influence on the line intensity ratio in Mössbauer spectra [6]. In order to investigate this behavior in more detail, Mössbauer spectroscopy on cyclic loaded ARMCO iron samples was performed at room temperature after stress-controlled fatigue loading. The samples were covered with a lead aperture (1 cm $\times$ 1 cm) to explore the magnetic structure of the specimen in the area where the macroscopic necking occurs (see Fig. 1, red square). The spectra were recorded by the use of the miniaturized Mössbauer spectrometer (MIMOSII, manufactured by SPESI, Space and Earth Science, Instrumentation, Ortenberg, Germany, [7]) mounted 2 ($\pm$ 1) mm above the sample. The MIMOS II Ti holder with Be window was equipped with a ^{57}Co Mössbauer source in Rh matrix with an active diameter of 4.5 mm. The emitted γ-rays penetrate the sample perpendicular to the sample surface (as shown in Fig. 1, red cross) after passing the lead aperture. The resonantly scattered 14.4 keV γ-rays were detected in backscattering geometry.

Regarding the analysis of the Mössbauer spectra, we concentrated on the detailed description of the line intensity ratio of the obtained magnetic six-line pattern. Thickness and geometry effects can lead to a broadening of the lines and thereby hinder the detailed comparison of the line intensities by variation of both, line width and line intensity. Therefore, we used the static Hamiltonian approach with only one fixed absorber line width, performing the analysis by least-square fitting procedure implemented in the Software WinNormos 3.0 for IGOR Pro (version 6.37) [8].

In addition, the dynamic properties of reference sample **1** and of the monotonically loaded specimen **2** were investigated by Nuclear Inelastic Scattering, performed at the 'High Resolution Dynamics Beamline P01' at PETRA III, DESY in Hamburg, Germany. The

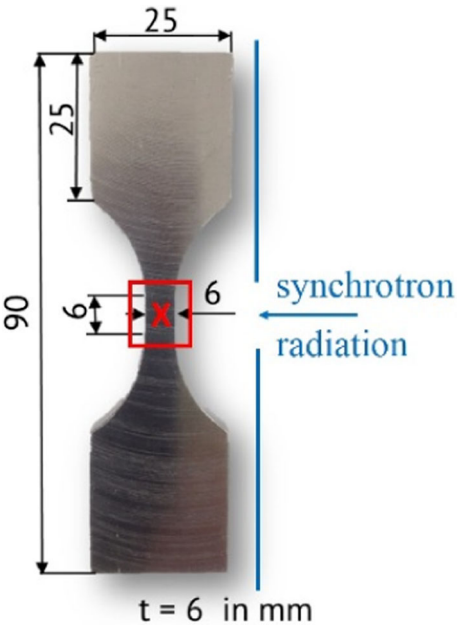

Fig. 1 Picture with dimensions of an ARMCO iron sample in its initial state **1**. The sample was equipped with a lead aperture in order to investigate the sample in the area where the macroscopic necking due to the loading occurs. The red square (blue lines) shows the lead aperture used during the conventional Mössbauer (NIS) experiments. The red cross indicates that the direction between the γ-rays and the sample surface was 90° during the Mössbauer experiments. The direction of the synchrotron radiation for the performance of the NIS experiments is depicted as a blue arrow. The sample was tilted by a few degrees (rotation along the longest axis of the sample)

Table 1 Overview of the mechanically loaded ARMCO iron samples*

	Mechanical loading	Details
1	Reference Sample	(See Fig. 1)
2	Monotonic	Just before failure, plastic strain ε_p =32.5%
3	Monotonic	After failure
4	Cyclic	$N_f = 1000$, just before failure (macroscopic necking)
5	Cyclic	$N_f = 1200$, after failure, fatigue

*The ultimate strength of the monotonic tensile test was 300 MPa. The stress-controlled fatigue test was performed with a constant stress amplitude $\sigma_a = 220$ MPa, load ratio $R = -1$ and frequency $f = 0.01$ Hz with N_f cycles at ambient temperature [6]

samples were also equipped with a lead aperture (Fig. 1) and the scattered radiation was detected by an avalanche photodiode mounted near (≈ 1 cm) above the sample. For the collection of the NIS data, the energy was tuned with a monochromator-setup around the resonance energy of 14.4 keV in a range of approximately -50 to 50 meV (step size 0.25 meV, energy resolution ≈ 1 meV). The experimentally determined density of vibrational states was generated using the method of double Fourier transformation to eliminate the multiphonon contribution together with the data deconvolution [5, 9]. The pDOS is further on calculated theoretically, employing classical molecular dynamics simulations using the open-source LAMMPS code [10] and the Fe atom interaction potential provided by Mendelev et al. [11].

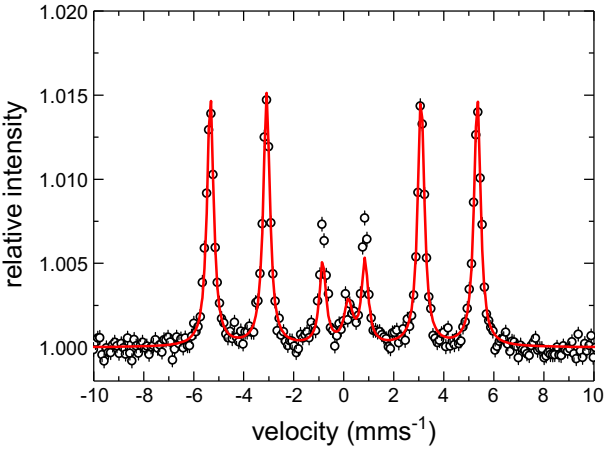

Fig. 2 Mössbauer spectrum of investigated polycrystalline ARMCO iron specimen **1**. The small singlet is due to iron impurities in an aluminum containing shielding that has not been used during the other measurements reported here. Red solid lines show theoretical simulations using the static Hamiltonian approach with $B_{hf} = 33.1\ (\pm 0.2)$ T, $\Gamma = 0.31\ (\pm 0.01)$ mms^{-1} and $\theta = 68\ (\pm 2)^\circ$

3 Results and discussion

The Mössbauer spectrum obtained at room temperature in reflection mode of the unloaded ARMCO iron sample **1** is shown in Fig. 2. The analysis reveals a magnetic hyperfine field of $B_{hf} = 33.1\ (\pm 0.2)$ T with zero isomer shift and quadrupole splitting. The theoretical relative intensities of the resonance lines are given by the probabilities of the treated nuclear transition. For the magnetic dipole transition (M1) in ^{57}Fe in the case of an unpolarized single line source, the line intensity ratio is given by 3:x:1:1:x:3. For a powder sample, the Zeeman pattern shows a characteristic magnetic pattern with 3:2:1:1:2:3 [12]. Such a random distribution is obviously not observed in the Mössbauer spectra of sample **1**, as the 2nd and 5th line are more intense than the first and the last one (see Fig. 2). This indicates a magnetic texture, i.e. a spatial angular distribution of the hyperfine magnetic field that leads to an average line intensity x. The average angle θ between the direction of the hyperfine magnetic field and the direction of the γ-rays is defined by $\cos^2(\theta) = (4 - x)/(4 + x)$ [13, 14]. A powder line intensity pattern of 3:2:1:1:2:3 can be obtained when θ is set to the so-called magic angle of 54.7° [8, 12, 15]. An alternative to the description with an average angle θ is the definition of the average square of the cosine $<(\boldsymbol{\gamma}\cdot\boldsymbol{m})^2>$, whereas $\boldsymbol{\gamma}$ and $\boldsymbol{m}$ are the unit vectors along the hyperfine magnetic field and the direction of the γ-rays [16]. The corresponding $<(\boldsymbol{\gamma}\cdot\boldsymbol{m})^2>$ values for all spectra are given in the Supplementary Material (Table S1).

In this way, the Mössbauer spectrum of specimen **1** is theoretically reproduced with $\theta = 68\ (\pm 2)^\circ$ proving the small texture of the ARMCO iron specimen (see Fig. 2).

The slight misfit of the theoretical simulation for the 3th and 4th line results from the restriction of the ratio of 3:1 for the intensities of the 1st and 3th line with fixed line width. Furthermore, it has to be noted that the analysis of an α-iron calibration foil with the static Hamiltonian approach reveals an angle of 60 $(\pm 1)^\circ$. Both deviations can result from thickness and geometry effects arising in the backscattering experiment using MIMOSII. Consequently, in the present study, we treat θ as a qualitative parameter to compare the

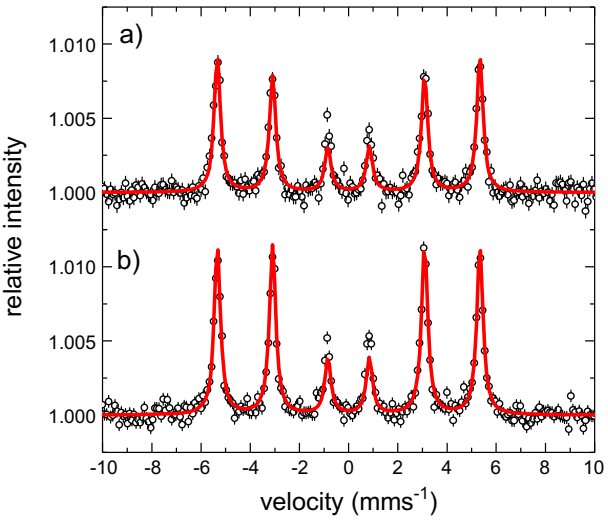

Fig. 3 Mössbauer spectra of monotonic loaded polycrystalline ARMCO iron specimen **a** just before ($\varepsilon_p = 32.5\%$, **2**) and **b** after failure (**3**). Solid lines show theoretical simulations using the static Hamiltonian approach with $B_{hf} = 33.1\ (\pm 0.2)$ T, **a** $\Gamma = 0.31\ (\pm 0.01)$ mms^{-1}, $\theta = 62\ (\pm 2)^\circ$ and **b** $\Gamma = 0.31\ (\pm 0.01)$ mms^{-1}, $\theta = 68\ (\pm 2)^\circ$

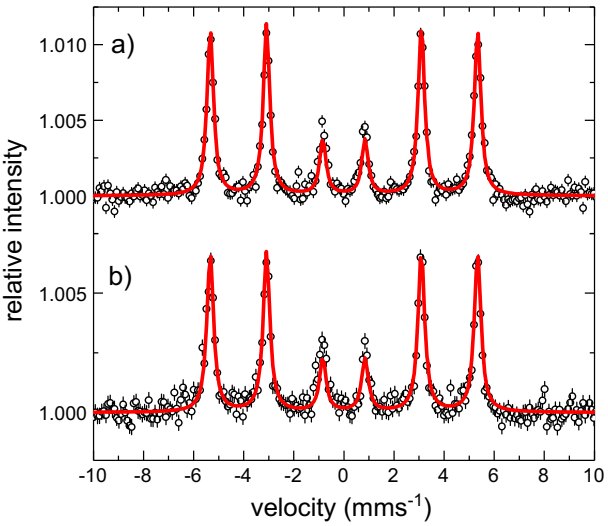

Fig. 4 Mössbauer spectra of cyclic loaded polycrystalline ARMCO iron specimen **a** just before (**4**) and **b** after failure (**5**). Solid lines show theoretical simulations using the static Hamiltonian approach with $B_{hf} = 33.1\ (\pm 0.2)$ T, **a** $\Gamma = 0.31\ (\pm 0.01)$ mms^{-1}, $\theta = 69\ (\pm 3)^\circ$ and **b** $\Gamma = 0.31\ (\pm 0.01)$ mms^{-1}, $\theta = 68\ (\pm 3)^\circ$

influence of loading on the ARMCO iron samples assuming the same thickness/geometry effects for all the samples **1** to **5**.

The Mössbauer spectra of the monotonic and cyclic loaded samples (Figs. 3 and 4) show that the plastic deformation reached in the tensile test also influences the magnetic texture. The Mössbauer spectrum of the specimen just before failure (see Fig. 3a, sample **2**) exhibits

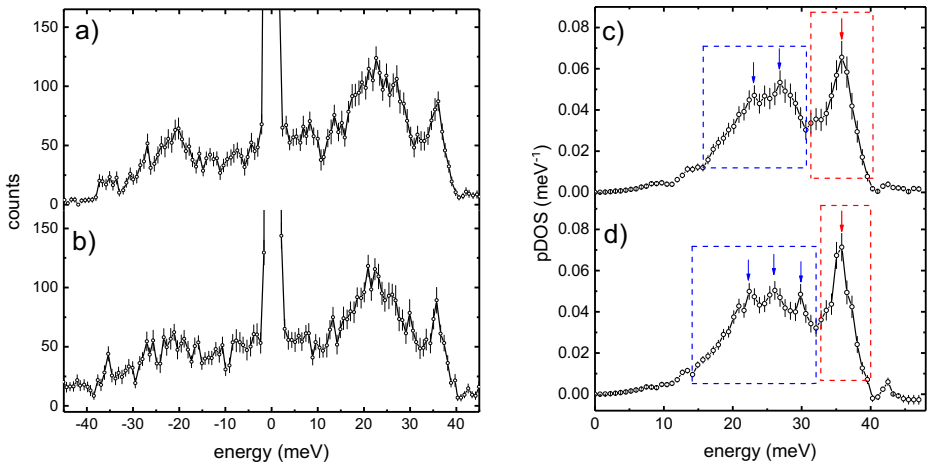

Fig. 5 NIS (left) and pDOS (right) of ARMCO iron specimen **a** and **c** before (sample **1**) and **b** and **d** after monotonic tensile test (sample **2**). The NIS data consists of several scans, summed up by a binning of 0.75 meV. Due to the lower statistical accuracy of the annihilation part (negative energy), the pDOS of sample **2** is extracted only from the positive part of the NIS spectrum [9]. The differences in the shape and sharpness of the pDOS of sample **1** and **2** are highlighted separating two energy regions (blue, red). The structures above 42 meV in the calculated pDOS are probably residuals arising from the deconvolution procedure [17]

an average angle of $\theta = 62\ (\pm 2)^\circ$ that is smaller than for the reference specimen **1**. Interestingly, the line intensity ratio of the monotonic loaded sample after failure (see Fig. 3b, sample **3**) shows with $\theta = 68\ (\pm 2)^\circ$ nearly the same pattern as the initial state specimen **1**. Consequently, despite the reported change of the magnetic flux density in the failure zone during specimen failure (0.26 mT [6]), there is no remarkable change of the magnetic texture detectable.

The spectra of the cyclic loaded samples (see Fig. 4) are slightly different from the monotonic loaded ones (Fig. 3). In particular, the type of loading (monotonic or cyclic) influences the change in the line intensity ratio. For the cyclic loaded specimen just before failure (sample **4**), there is no decrease but a slight increase of θ (see Fig. 4a, $\theta = 69\ (\pm 3)^\circ$). The spectrum of the specimen after failure (**5**) exhibits within the error bars again nearly the same line intensity ratio as the one of sample **1** (see Fig. 4b, $\theta = 68\ (\pm 3)^\circ$). Consequently, this Mössbauer study shows that the mechanical loading of iron as a ferromagnetic material leads to a tiny change in the magnetic texture. The detailed correlation of these effects with the influence of monotonic and cyclic loading on the bulk, crystallographic as well as the magnetic micro-, structure will be a subject of further investigations.

The influence of monotonic tensile testing with regard to the dynamic properties was further investigated, performing NIS experiments on samples **1** and **2**. The experimentally obtained NIS spectra of both specimens show one broad sideband centered at round about 23 meV and one small band at 36 meV in the phonon creation region. The same peaks with lower intensities are also observable in the negative energy range (phonon annihilation) (see Fig. 5a, b). This band-structure is in excellent agreement to previously reported NIS spectra of α-iron [5, 9, 17].

The comparison of the experimentally determined pDOS for both samples shows that slight differences in the pDOS pattern occur (see Fig. 5c and d). Especially in the range of 15 meV to 32 meV (blue marked region), the pDOS of sample **2** displays several distinct

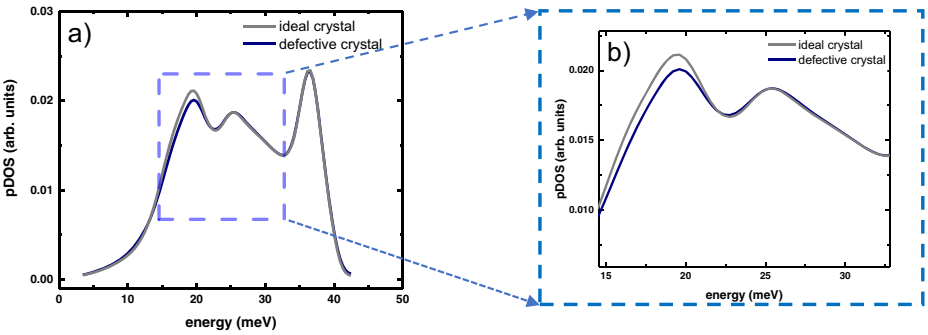

Fig. 6 **a** By means of classical molecular dynamics calculated pDOS of a reference Fe crystallite (ideal crystal, gray) and a crystal containing a large density of dislocations (defective crystal, dark blue), **b** enlarged section of the pDOS to highlight the effect of dislocations

Table 2 Properties of ARMCO iron at room temperature determined by means of the pDOS, calculated from the experimental NIS spectra: Lamb-Mössbauer factor f_L, mean-square displacement $|x|$, mean internal energy U, specific heat c_v, entropy S, mean energy G and normalized mean force constant D

	f_L	$\|x\|$ (Å)	U (meV)	c_v (k_B)	S (k_B)	G (meV)	D (N/m)
	0.791(6)		*83.4(15)*	*2.70(3)*	*3.00(3)*		*185(12)*
1	0.790 (±0.01)	0.115 (±0.005)	85.23 (±1)	2.72 (±0.03)	3.10 (±0.1)	27.5 (±3)	177 (±8)
2	0.787 (±0.02)	0.116 (±0.005)	84.87 (±3)	2.73 (±0.08)	3.16 (±0.3)	26.9 (±5)	168 (±15)

The given error bars are due to the pDOS calculation procedure. Reference parameters are given in italic [19]

bands (at 22.4, 26.1 and 29.8 meV) instead of two bands observable in the pDOS of sample **1** (small peaks at 23.1 and 26.9 meV). In fact, a three band-structure was already observed in a theoretically calculated pDOS by means of molecular dynamics simulations for bcc-Fe [18]. However, these calculations have not taken stress or fatigue into account. The preliminary molecular dynamics simulations presented in this work (see below, Fig. 6) only show a two-band-structure. However, it cannot be excluded, that the experimentally observed three-band structure is influenced by the low signal to noise ratio. The origin of this structure will be subject to further combined experimentally and theoretically investigations.

Furthermore, there are also differences observable in the shape and sharpness of the peak at 35.8 meV (red area). The peak intensity in the pDOS of specimen **2** is increased by 0.1 meV^{-1} ($\approx +13\%$) accompanied by a decrease of the full width at half-maximum ($\approx -24\%$) compared to the peak in the pDOS of the reference sample **1**. This behavior is opposite to the reported pressure-induced decrease of this mode in iron [19]. An analogous pressure-induced behavior was also reported for Fe in $DyFe_3$ [20].

From the integral properties of the phonon DOS, some thermodynamic parameters as Lamb-Mössbauer factor f_L, mean-square displacement $|x|$, mean internal energy U, specific heat c_v, entropy S, mean energy G and the normalized mean force constant D can be extracted (see Table 2) [5]. All determined parameters for both specimen show a good agreement of the properties with reported values for α-iron [17, 19]. The comparison for the parameters of sample **1** and **2** yields no pronounced differences with exception

of the temperature independent mean force constant D. The determined mean force constant of specimen **2** with $D = 168\ (\pm 15)$ N/m is slightly lower[1] than for sample **1** ($D = 177\ (\pm 8)$ N/m). This influence of tensile deformation may be indeed expected since in high pressure NIS experiments on α-iron an increasing mean force constant is observed (185 ($\pm$ 12) N/m at 0 GPA, 279 ($\pm$ 25) N/m at 6 GPa [19, 21]).

Summarizing, the experimentally determined NIS spectra and the extracted pDOS reveal an influence of a monotonic tensile test on the dynamic properties of ARMCO iron. In order to examine the effect of plasticity on the pDOS, we additionally employed classical molecular dynamics (MD) simulations. As a reference, we use a Fe crystallite containing around 432000 atoms in a single-crystal structure. Defects are introduced by loading the crystal with a high number of dislocations; after relaxation, the dislocation density amounts to $4.8{\cdot}10^{12}$ cm^{-2}. The pDOS, shown in Fig. 6, is calculated from the velocity autocorrelation of the samples at low temperature ($T < 1$ K), in order to minimize thermal effects. The defective crystal shows a changed spectrum in particular in the region of the first peak, at around 20 meV, which is caused by the lowest-energy transversal acoustic phonons at the Brillouin-zone boundary.

The results presented here reflect a starting point of further experiments and MD calculations, which will shed light on the interplay of magnetic and vibrational effects occuring during monotonic and cyclic loading of iron containing engineering materials.

Acknowledgemnents This work has been supported by the German Research Foundation (DFG) within the SFB/TRR 173 "SPIN+X" and by DESY via experiment No. 11001564. The authors thank Dr. R. A. Brand from the University of Duisburg for his support using the WinNormos Software

References

1. Davis, J.R.: Tensile Testing, Materials Park. ASM International, Ohio (2004)
2. Dowling, N.E.: Mechanical behavior of materials: engineering methods for deformation, fracture, fatigue. Pearson, Boston (2012)
3. Perevertov, O.: Influence of the residual stress on the magnetization process in mild steel. J. Phys. D.: Appl. Phys. **40**, 949–954 (2007)
4. Grad, P., Reuscher, B., Brodyanski, A., Kopnarski, M., Kerscher, E.: Mechanism of fatigue crack initiation and propagation in the very high cycle fatigue regime of high-strength steels. Scripta Materialia **67**, 838–841 (2012)
5. Chumakov, A.I., Sturhahn, W.: Experimental aspects of inelastic nuclear resonance scattering. Hyp. Interact. **123/124**, 781–808 (1999)
6. Smaga, M., Scherthan, L., Auerbach, H., Wolny, J.A., Schünemann, V., Beck, T.: Magneto-mechanical behavior of iron during monotonic and cyclic loading. Solid State Phenomena **258**, 456–459 (2017)
7. Klingelhöfer, G., Morris, R.V., Bernhardt, B., Rodinov, D., de Souza, P.A. Jr., Squyres, S.W., Foh, J., Kankeleit, E., Bonnes, U., Gellert, R., Schröder, C., Linkin, S., Evlanov, E., Zubkov, B., Prilutski, O.: Athena MIMOS II Mössbauer spectrometer investigation. J. Geohphys. Res. **108**, 8067 (2003)
8. Brand, R.A.: Winnormos-For-Igor, 3.0. University Duisburg, Duisburg (2009)
9. Kohn, V., Chumakov, A.: DOS: Evaluation of phonon density of states from nuclear resonant inelastic absorption. Hyperfine Interact. **125**, 205–221 (2000)
10. Slimpton, S.: Fast parallel algorithms for short-range molecular dynamics. J. Comput. Phys. **117**, 1–19 (1995)

[1]The error bars are relatively large due to the occurring differences in the pDOS extraction procedure, depending on the exact way of background, multi-phonon-contribution and central elastic peak subtraction. The reported decreasing tendency of D occurs independent of this pDOS calculation procedure.

11. Mendelev, M., Han, S., Srolovitz, D.J., Ackland, G.J., Sun, D.Y., Asta, M.: Development of new interatomic potentials appropriate for crystalline and liquid iron. Phil. Mag. **83**, 3977–3994 (2003)
12. Gütlich, P., Bill, E., Trautwein, A.X.: Mössbauer Spectroscopy and Transition Metal Chemistry. Springer, Berlin (2011)
13. Keune, W.: Application of Mössbauer spectroscopy in magnetism. Hyp. Interact. **204**, 13–45 (2012)
14. de Oliveira, L., da Cunha, J.B.M., Spada, E.R., Hallouche, B.: Mössbauer spectroscopy and magnetic properties in thin films of Fe_xNi_{100-x} electroplated on silicon (1 0 0). Appl. Surf. Sci. **254**, 347–350 (2007)
15. Madsen, M.B., Bertelsen, P., Goetz, W., Binau, C.S., Olsen, M., Folkmann, F., Gunnlaugsson, H.P., Kinch, K.M., Knudsen, J.M., Merrison, J., Nornberg, P., Squyres, S.W., Yen, A.S., Rademacher, J.D., Gorevan, S., Myrick, T., Bartlett, P.: Magnetic Properties Experiments on the Mars Exploration Rover Mission. J. Geophys. Res. **108**, 8069 (2003)
16. Olszewski, W., Szymański, K., Satula, D., Dobrzyński, L.: Magnetic texture determination by CEMS with polarized radiation. Nukleonika **52**, 17–19 (2007)
17. Sturhahn, W., Toellner, T.S., Alp, E.E., Zhang, X., Ando, M., Yoda, Y., Kikuta, S., Seto, M., Kimball, C.W., Dabrowski, B.: Phonon density of states measured by inelastic nuclear resonant scattering. Phys. Rev. Lett. **74**, 3832–3835 (1995)
18. Talati, M., Posselt, M., Bonny, G., Al-Motasem, A., Bergner, F.: Vibrational contribution to the thermodynamics of nanosized precipitates: vacancy-copper clusters in bcc-Fe. J. Phys.: Condens. Matter **24**, 225402–225410 (2012)
19. Lübbers, R.: Magnetism and Lattice Dynamics Under High Pressure Studied by Nuclear Resonant Scattering of Synchrotron Radiation. Dissertation University Paderborn (2000)
20. Tanis, E.A.: Partial phonon density of states of 57-iron and 161-dysprosium in $DyFe_3$ by nuclear resonant inelastic X-ray scattering under high pressure. University of Nevada, Las Vegas: Master Thesis (2010)
21. Shen, G., Sturhahn, W., Alp, E.E., Zhao, J., Toellner, T.S., Prakapenka, V.B., Meng, Y., Mao, H.-R.: Phonon density of states in iron at high pressures and high temperatures. Phys. Chem. Minerals **31**, 353–359 (2004)